

Investigation Effect of Magnet Skew on Thrust Force in Linear Brushless Direct Current Motor with FEM

Mustafa Eker ^{a,1}

^a Electrical and Electronics Engineering, Institute of Graduate Studies, Tokat Gaziosmanpasa University, Tokat, Turkey
ORCID ID: 0000-0003-1085-0968

Abstract

This study is concerned with the reduction of ripple in the thrust force produced in a linear Brushless Direct Current Motor (BLDC). To reduce the ripples in the generated thrust force, different methods such as structural solutions are applied both in the control part and in the production phase of the motor. In this study, skew application, which is one of the mechanical methods, is proposed. For this reason, the changes in the thrust force of a BLDC motor with a surface magnet-placed translator are investigated by applying different levels of skew to the magnets. First, a 3D solid model of the motor was created. A pole on the translator of the linear BLDC motor is composed of 3 equal magnet groups. For each skew level, the magnets were shifted 3 mm independently of each other and the thrust force values were examined. For this process, a 3D magnetostatic analysis of the linear BLDC motor was performed. The results obtained show that the skewing process applied to the magnets reduces the ripples in the thrust curve up to a certain point, after which no significant improvement in the ripple is observed, while the average force value decreases significantly.

Keywords: “Linear BLDC, thrust force, ripple, step skew.”

1. Introduction

Considering energy efficiency in recent years, the aim is to achieve low energy consumption and high performance from electrical machines. Therefore, it is aimed to use structures with high acceleration, precise position control, simpler structure, and low maintenance for this process. One of the structures that provide these features is the linear motor structure[1]–[3]. Although the history of linear motors dates to ancient times, their usage areas have started to increase gradually nowadays. Linear motors have different types like rotary machines. One of these types is the linear Brushless Direct Current Motor (BLDC), which is included in the group containing magnets. Linear BLDC motors are frequently preferred in speed, acceleration, and position-controlled drive systems such as CNC machines, robotics and automation applications, rocket positioning systems, gene sequencing, conveyor systems, crane systems and magnetic levitation, electromagnetic maneuvering, high-speed transportation, etc[4], [5].

Linear BLDC motors are produced in different structures and are defined by various names[5], [6]. Depending on the number of stator/translators, and magnet position, various definitions are used in literature [4], [7]. They can also be named according to whether the cores used are slotted or slotless. In general, a linear BLDC motor is also defined as a simple structure. The most obvious advantages of linear BLDC motors are that the stator windings and general structure are easy to install, the air gap can be adjusted more easily than radial motors, the end winding resistance is short, and the flux distribution has lower harmonics.

One of the main disadvantages of linear BLDC motors is the ripples in the generated forces. These force ripples are mainly caused by cogging force and mutual force. The flux density function of the magnets used in the Linear BLDC motor is not always uniform, so ideal square wave and trapezoidal wave are not formed. In addition, the magnets are not endless structures but have corner points. These corners cause deviations in the flux distribution towards the end. In addition, due to the slotted structure, the reluctance value changes, and this causes distortions in the flux distribution. These distortions cause ripples in the generated thrust and pulling forces.

Various methods have been proposed and applied to minimize the force ripples that occur in a linear BLDC motor in [8]–[13]. Some of these methods are aimed at reducing the ripple value by modifying the structure of the motor. The process of

¹ Corresponding Author
E-mail Address: mustafa.eker@gop.edu.tr

skewing the magnets is one of these methods. Generally, magnets are produced by skewing during the production phase and mounted on the translator. This increases the production cost and causes problems in the possible procurement process. Another method is to reduce the ripple value with step skewing. This study aims to reduce the torque ripple in the thrust force of the linear motor with a step skew. For this reason, the magnets in the translator are subjected to a skewing process.

This study consists of 5 sections. First, there is the Introduction section, then the structure and working principle of the preferred motor are given. Section 3 presents the mathematical expressions for the linear BLDC motor and the solution to the problem. Section 4 describes the modeling of the motor and the FEM process. Results are given in the Result section and evaluation is made in the Conclusion section.

2. Basic Working Principle and Structure of Linear BLDC Motor

In their simplest form, linear motors can be defined as the linearized state of a rotary motor cut along its radius. The operation of a linear motor has the same principle as that of a rotary machine. However, in the linear motor, the torque expression used in rotary machines is replaced by the force expression. The Fig. 1 shows the basic view of the single-sided linear BLDC and the 3D solid model of the proposed structure[14].

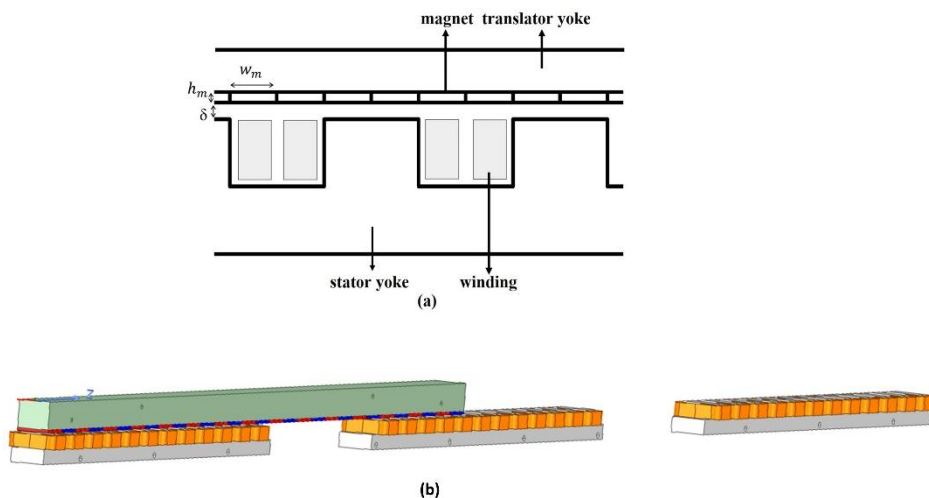


Fig. 1. a) The basic view of the single-sided Linear BLDC b) 3D solid model of the proposed model

The working principle of the linear motor is basically similar to rotary machines. However, while the output parameter in rotary machines is defined by torque, the equivalent of this expression in linear machines is given as force. Linear BLDC motors could move with a trapezoid DC excitation. BLDC motors are operated with the excitation of two phases of a 3-phase source. For linear BLDC motors to move, it is very important to determine the rotor position relative to the stator. It is a necessary condition for the excitation of the appropriate windings. The use of hall sensors to determine the position is a very common method.

Two of three phases are excited to drive the BLDC motor driving system. There is just one mode of operation for two switches. Three-phase stator windings are assumed to be symmetrically star-connected and the parameters are assumed to be constant, also assuming that the values of self and mutual inductance do not change, the 3-phase voltage equation is as follows[15];

$$\begin{bmatrix} u_a \\ u_b \\ u_c \end{bmatrix} = \begin{bmatrix} R_a & 0 & 0 \\ 0 & R_b & 0 \\ 0 & 0 & R_c \end{bmatrix} \begin{bmatrix} i_a \\ i_b \\ i_c \end{bmatrix} + \begin{bmatrix} L_a & M & M \\ M & L_b & M \\ M & M & L_c \end{bmatrix} \frac{d}{dt} \begin{bmatrix} i_a \\ i_b \\ i_c \end{bmatrix} + \begin{bmatrix} e_a \\ e_b \\ e_c \end{bmatrix} \quad (1)$$

Some assumptions are made when generating the equivalent circuits of the motors. For BLDC, it is assumed to be operated at rated conditions with star winding connection. In this way, the current-induced saturation effect is neglected. Stator resistances of all windings are equal, self, and mutual inductances are taken constant and iron losses are neglected. With these assumptions, BLDC can be represented as follows.

$$u_a - u_o = R_a \cdot i_a + \frac{d(L_a \cdot i_a + M \cdot i_b + M \cdot i_c)}{dt} + e_a \quad (2)$$

$$u_b - u_o = R_b \cdot i_b + \frac{d(M \cdot i_a + L_b \cdot i_b + M \cdot i_c)}{dt} + e_b \quad (3)$$

$$u_c - u_o = R_c \cdot i_c + \frac{d(M \cdot i_a + M \cdot i_b + L_c \cdot i_c)}{dt} + e_c \quad (4)$$

Where u_a, u_b, u_c , are the phase winding voltages, phase resistances a, b, and c are denoted R_a, R_b , and R_c respectively. The currents of phases a, b, and c are given i_a, i_b ve i_c respectively and the self-inductances are given by L_a, L_b ve L_c . M the mutual inductance and e_a, e_b ve e_c are the back emf values. Equation 5 gives u_o which is the differential voltage between the star connection point of the windings and the power stage natural zero and is expressed fallows,

$$u_o = \frac{1}{3} \sum_{j=a,b,c} u_j - \sum_{j=a,b,c} e_j \quad (5)$$

In 3-phase systems, the sum of the three phase current values is assumed to be zero. Also, considering the concentrated winding configuration, the mutual inductance is negligibly small. Also, with the above-mentioned assumptions, if Equations 2-4 are rewritten;

$$u_a - u_o = R_a \cdot i_a + L_a \frac{di_a}{dt} + e_a \quad (6)$$

$$u_b - u_o = R_b \cdot i_b + L_b \frac{di_b}{dt} + e_b \quad (7)$$

$$u_c - u_o = R_c \cdot i_c + L_c \frac{di_c}{dt} + e_c \quad (8)$$

If the electromagnetic force F_e expression is written from these expressions.

$$F_e = \frac{e_a \cdot i_a + e_b \cdot i_b + e_c \cdot i_c}{v} \quad (9)$$

Motor speed depends on the interaction of the electromagnetic force and the force due to the load. Equation 10 can be written for the motor speed,

$$m \frac{dv}{dt} = F_e - F_{load} - D \cdot v \quad (10)$$

Where D is the damping coefficient, m is the mass, F_{load} is the load force and v is the speed. For rotating machine considering motor dynamics,

$$T_m = J \frac{d\omega}{dt} + T_{load} - B \cdot \omega \quad (11)$$

The torque expression can be written as Equation 11. If this motion is rewritten for one dimension, the Equation 12 for linear machines is obtained.

$$F_m = m \frac{dv}{dt} + F_{load} + D \cdot v \quad (12)$$

$$F_m(s) = s \cdot m \cdot v(s) + F_{load}(s) + D \cdot v(s) \quad (13)$$

The equation 13 gives the motor dynamics in the frequency domain. Where $F_m(s), F_{load}(s)$ and $v(s)$ represent the laplace transforms of F_m, F_{load} and v respectively.

From the dynamic equation of the motor, it is observed that mass, friction force, and load force act on the moving part. So far, the electrical formulation is given the basic equations of the DC motor and includes the nonlinear dynamics. These equations make some assumptions. Some of these assumptions are that the magnetic circuit is linear, and the friction force is always constant. The BH characteristics of the motor parts do not change linearly. For example, the saturation of the material is not the same in all regions and the magnetic behavior changes completely due to the saturation point. On the other hand, it is assumed that the friction force does not change with motor speed and therefore only viscous friction exists. These values cause a small deviation from the actual results.

In DC motors the magnetic flux is generated by the stator windings. The stator will be assumed to have a single coil characterized by an inductance L_e due to the windings and a resistance R_e due to the distributions in the conductor. The equation for such an electrical circuit is given by,

$$V_e(t) = L_e \frac{di_e}{dt} + R_e \cdot i_e + e \quad (14)$$

If the Equation 10 is transformed in the Laplace domain of the signal assuming linearity;

$$\frac{i_e(t)}{V_e(t) - e} = \frac{K_e}{1 + T_e s} \quad (15)$$

It can be written as Equation 15. where $K_e = \frac{1}{R_e}$ is the stator gain and $T_e = \frac{L_e}{R_e}$ is the stator time constant.

3. Electromagnetic FEM Analysis

One of the methods used in the design/development of electrical machines is the FEM method. The design or state analysis of the linear BLDC motor can be obtained by FEM using some assumptions and limitations. The material properties of the motor parameters and the operating conditions of the motor are defined in the system. In this way, results can be developed in nonlinear situations. The accuracy of these solutions is directly related to the meshing process. With the mesh, the vector potential values of the motor parts can be calculated for each situation. Current sheets J used to give excitation in the stator winding [16],

$$\vec{J}(t) = J(t) \vec{k} \quad (16)$$

In magnetic field analysis, magnetic field strength \vec{H} and flux density \vec{B}

$$\vec{H} = \frac{1}{\mu} \vec{B} - \frac{1}{\mu} \vec{M}_0 \quad (17)$$

In the Equation 17, μ and M_0 represent the magnetic permeability of materials and the magnetization vector of permanent magnets, respectively. The flux value of the magnets and the rotor core is defined as a single value. In this way the Poissons Equation is expressed as Equation 18,

$$\frac{\partial}{\partial x} \frac{1}{\mu} \frac{\partial A}{\partial x} + \frac{\partial}{\partial y} \frac{1}{\mu} \frac{\partial B}{\partial y} = -(J + J_m) \quad (18)$$

In the Equation 18, the vector potential and current density corresponding to the magnets are A and J_m respectively. The current density is given by the Equation 19,

$$J_m = \text{rot}_z(\mu^{-1} \vec{M}_0) = \frac{\partial(\mu^{-1} \vec{M}_{0y})}{\partial x} \frac{\partial(\mu^{-1} \vec{M}_{0x})}{\partial y} \quad (19)$$

The calculated longitudinal force can be found using the volume integral of the vector product of the current sheet, J , and the flux density, B , as given in Equation (20).

$$\vec{F} = \int_v \vec{J} \times \vec{B} \cdot dV \quad (20)$$

There are three types of magnetic forces in an electric machine. The Lorentz force acting on the windings inside the magnetic field, the magnetostrictive force acting inside the iron core, and the reluctance force acting on material boundaries with different magnetic properties. The reluctance force of an electric motor is the electromagnetic force, which contains two components: radial and tangential components. In a two-dimensional SEY calculation, the material boundary is chosen as the edge of the stator end. The two components of the electromagnetic force can be calculated according to Equations 21 and 22 [17]:

$$F_{rad} = \frac{L_{stk}}{2\mu_0} \oint_l (B_n^2 - B_t^2) dl \quad (21)$$

$$F_{tan} = \frac{L_{stk}}{\mu_0} \oint_l B_n \cdot B_t dl \quad (22)$$

Where B_n and B_t are the normal and tangential component of the flux density respectively, l is the stator end edge length and L_{stk} is the length of the package length of the machine.

For FEM analysis, a 3D solid model of the motor was created, and material definitions were made. According to the equation, the force to be generated is related to the magnetic flux. Another factor affecting the magnetic flux is the type of material. For this reason, the BH curves of the materials were activated by defining the material in the solid model created. Some parameters and material type of the linear BLDC motor part are given in the Table 1.

Table 1. Linear BLDC motor parameters

Description	Value / definition
Supply voltage (V)	24
Axial length of each coil (mm)	30
One pole magnets length (mm)	30
Length of stator (mm)	480
Sum of length of stator (mm)	1920
Length of translator (mm)	900
Magnet width (mm)	10
Magnet length (mm)	30
Magnet thickness (mm)	2
Stator	M350 steel
Stator windings	Copper
Translator	AISI 1045 Steel
Magnets	N40SH

The accuracy of the results in FEM analysis is related to the number of meshes created in the materials. While the increase in the number of meshes is an important parameter in approaching the exact result, it causes an increase in the analysis time. For this study, fine mesh structure from standard mesh definitions was used. The obtained mesh structure is given in the Fig. 2. At the end of the meshing process, the total mesh is 984039 pieces, 271835 in the stator, 137863 in the translator, and 139539 in the magnets.

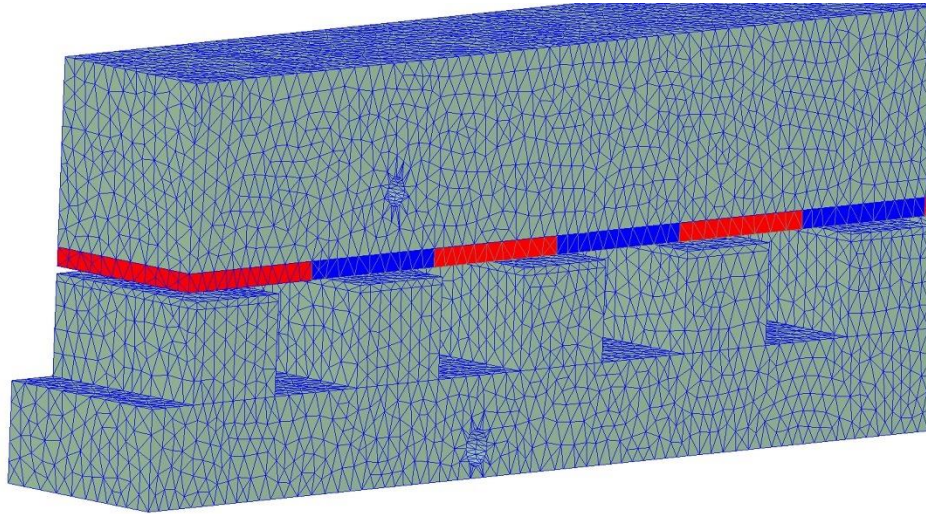


Fig. 2. Mesh structure

4. Proposed Method

In order to reduce ripple in thrust force in motors, different methods are used in the structural or driving method [18]–[21]. In this study, the step skew method is applied to the magnets in the translator to produce a solution in the structural methods. There are 3 equal magnets on one pole in the translator. One of these magnets is kept fixed and the other two magnets are shifted in the direction of the axis where the thrust force occurs at certain rates. The outside magnet was shifted at a maximum value of 30 mm.

This value corresponds to one magnet length. In the case of a maximum skew level, the magnet in the middle was shifted by 15 mm in the same axis and direction. Table 2 shows the nomenclature of the magnets according to the skew state. The Fig. 3 shows the image of the skewing process applied. Fig. 3a show the normal translator called step_0mm. Fig. 3b shows the image of the maximum shift called step_30mm.

Table 2. The nomenclature of the magnets according to the skew state

Skew denomination	1 st magnet	2 nd magnets	3 rd magnets
Step_0mm	Fixed	fixed	fixed
Step_3mm	Fixed	1.5 mm	3.0 mm
Step_6mm	Fixed	3.0 mm	6.0 mm
Step_9mm	Fixed	4.5 mm	9.0 mm
Step_12mm	Fixed	6.0 mm	12.0 mm
Step_15mm	Fixed	7.5 mm	15.0 mm
Step_18mm	Fixed	9.0 mm	18.0 mm
Step_21mm	Fixed	10.5 mm	21.0 mm
Step_24mm	Fixed	12.0 mm	24.0 mm
Step_27mm	Fixed	13.5 mm	27.0 mm
Step_30mm	Fixed	15.0 mm	30.0 mm

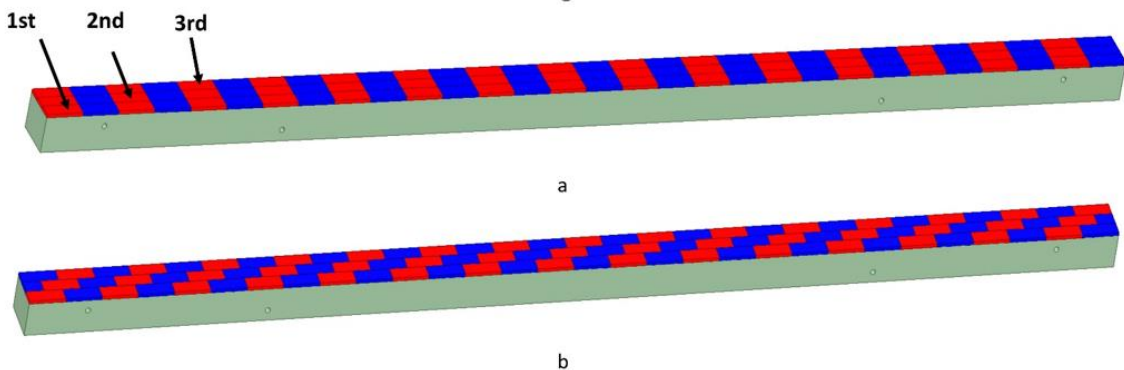


Fig. 3. Translator magnet states a) step_0mm b) step_30mm

5. Result

Technical information of the motor used is given in Table 1. The 3D solid motor was created in these dimensions, and the thrust force and pulling force occurring in the motor were examined by performing a FEM analysis. In Fig. 4, the thrust force curves of the structures without and with skew are given together. Fig. 5 shows the Fast Fourier Transform (FFT) plots of the force curves.

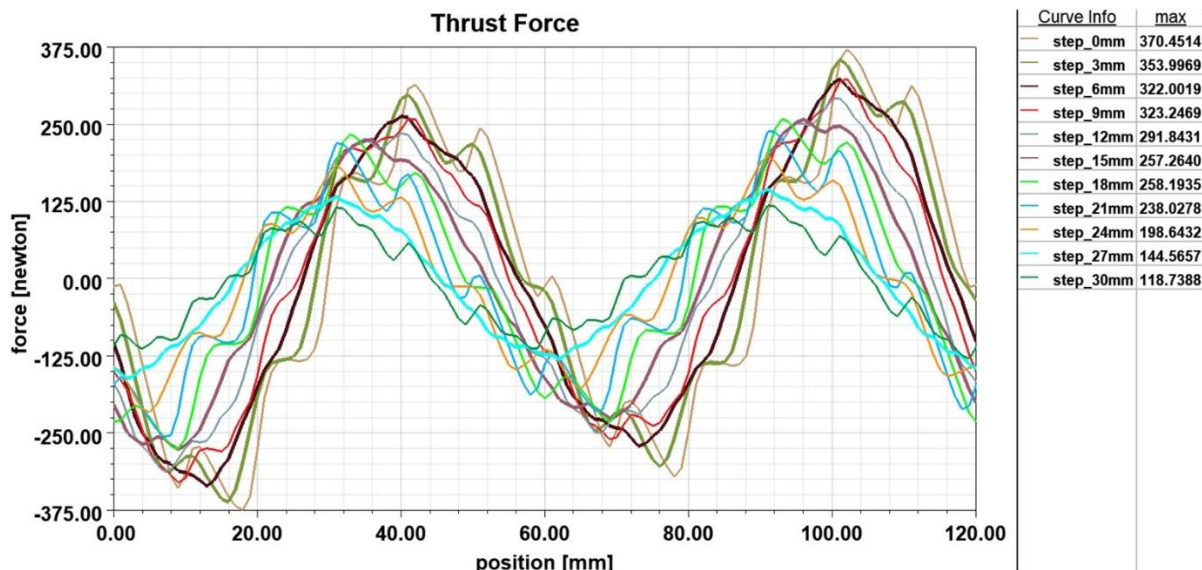


Fig. 4. Thrust force for all skew levels

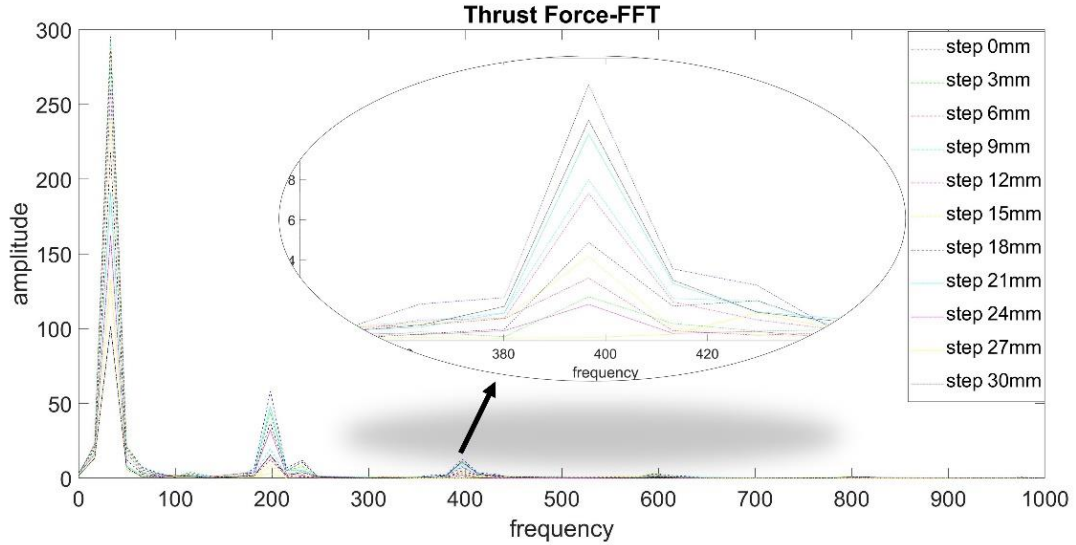


Fig. 5. FFT of thrust force

Fig. 4 shows the thrust curves produced by the linear BLDC motor for different skew values, and the FFT plots of these curves are given in Fig. 5. When the curves are analyzed, it is observed that the maximum value of the force decreases as the amount of skew increases. While the maximum force produced by the motor of the translator without skew is 370N, this value is obtained as 257N in the structure with 15 mm skew and 118N in the structure with 30 mm skew. The ripple values of the thrust force show improvement with the skew level. However, the decrease in the force value produced by the skew process shows that the optimum skew value should be determined. For this reason, FFT graphs of the force curves were obtained. The results show that the skew level reduces the ripples in the generated force curves. It is seen that the harmonics occurring due to ripples are reduced. When the graphs are analyzed, when the maximum force generated and the ripple values are evaluated together, it is seen that the structure with a 6 mm skew is the most suitable. Although the best harmonic is shown in the structure of 27 mm skew level, the force produced at this skew value is very low.

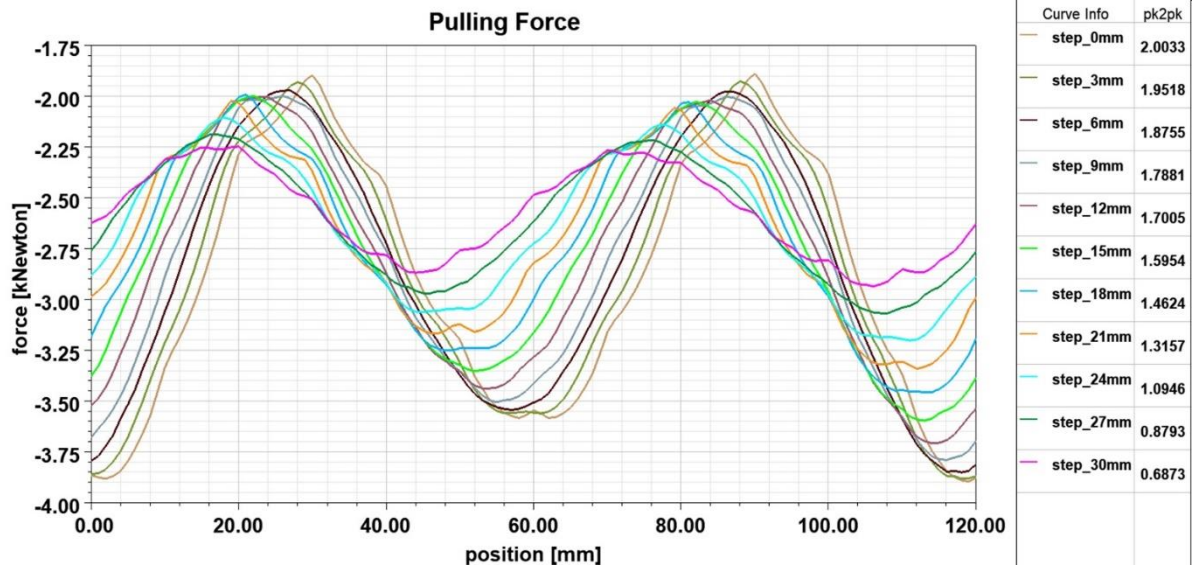


Fig. 6. Pulling force for all skew levels

Fig. 6 shows the curves of the pulling forces produced by the linear BLDC motor for different skew levels. Like the ripple value occurring in the thrust force, the ripple value occurring in the pulling force curve decreases with the skew effect. The same effect of the skew values, where successful results were obtained in thrust force value, also showed the same effect in pulling force value. In the average values of pulling force, a decrease from 2 kN to 0.6 kN was observed.

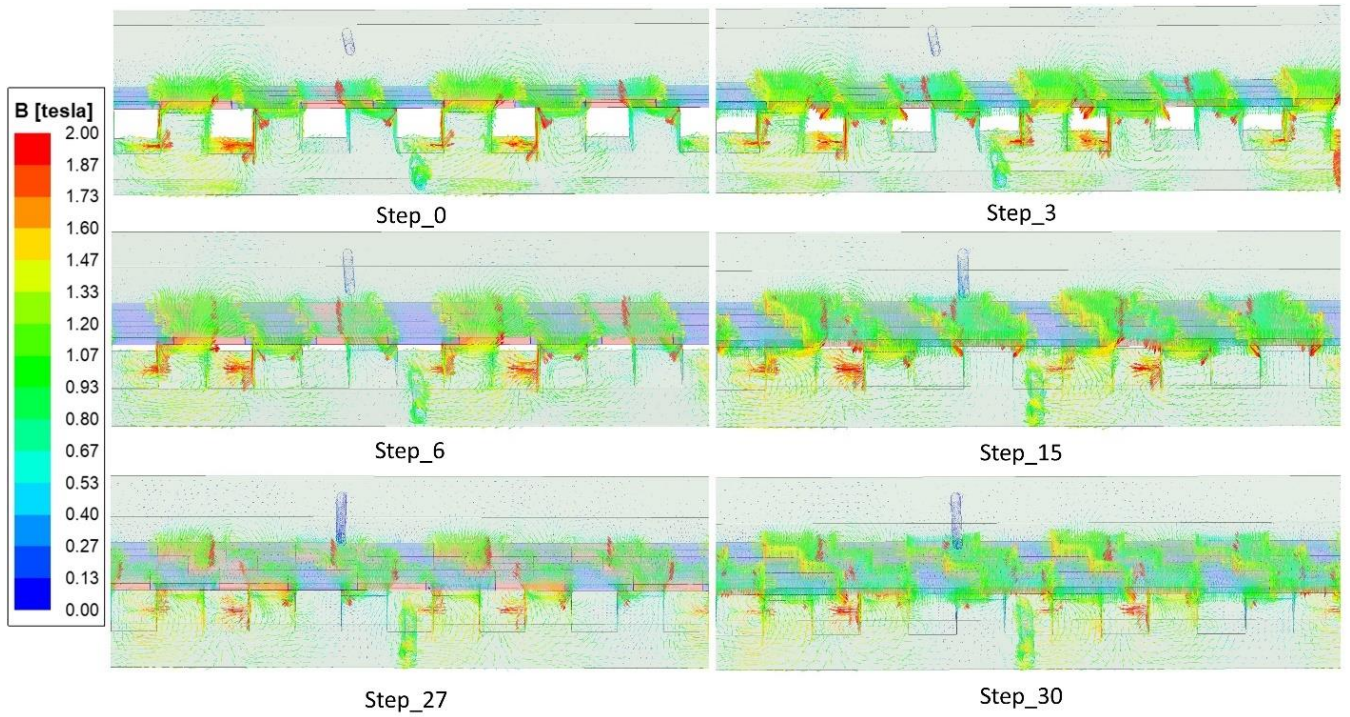


Fig. 7. Magnetic flux vector for some skew levels

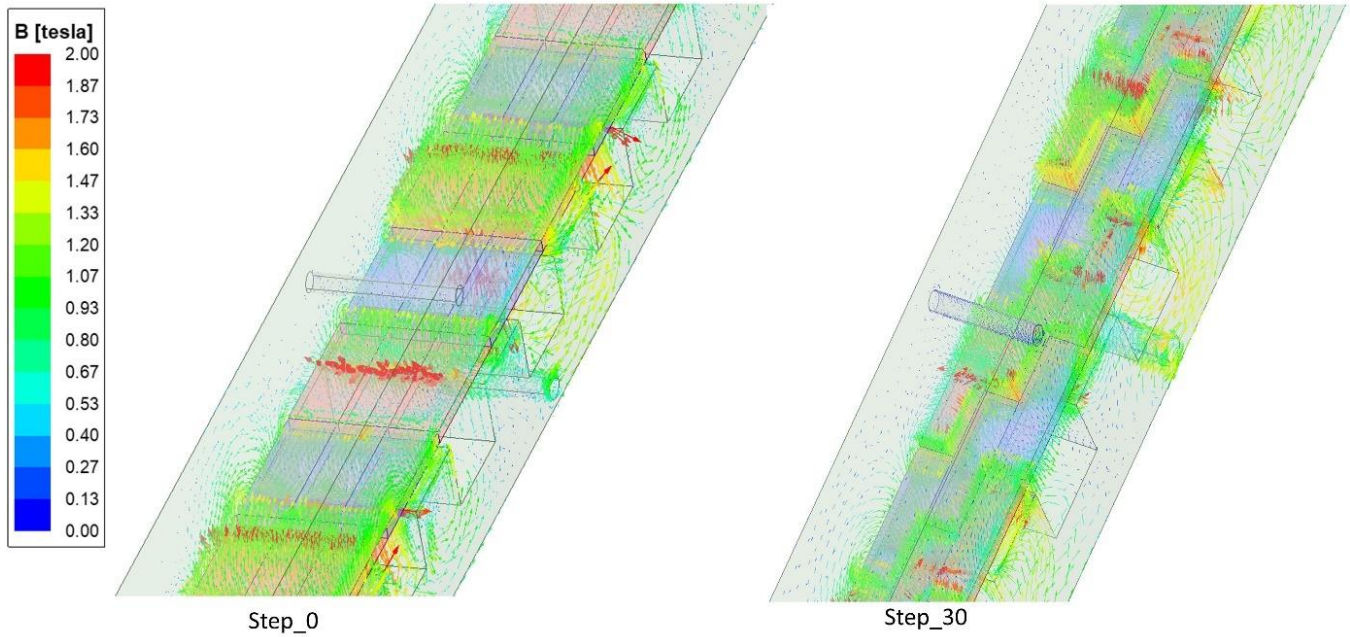


Fig. 8. Magnetic flux vector

Fig. 7 show the flux vectors generated in the motor for some skew levels. The distribution of the flux provided by the magnets at different levels of skew is also shown in detail in Fig. 8. When the figures are examined, it can be seen that the flux vectors produced according to each skew condition are displaced and therefore changes in the flux paths are realized. In this way, although there is a homogeneity in the flux distribution, there is a decrease in the forces generated. However, no negative saturation was observed for the materials in the flux density of the materials when examined in each case.

6. Conclusion

This study was carried out to reduce the ripples occurring in the thrust force of the linear BLDC motor. In this study, the process of skewing the magnets was applied. There are 3 equal magnets on one pole in the translator. One of these magnets is kept fixed and the other two magnets are shifted in the direction of the axis where the thrust force occurs at certain rates. The skew process was shifted by a maximum magnet length of 30 mm.

The results show that skewing reduces the ripples in the thrust force. The ripple values of the thrust force and pulling force improve with the level of skewness. The skew process improves the harmonics in the thrust and pulling curves of the motor. However, it also causes a decrease in the maximum and average values of the generated forces. When the curves are examined, the least harmonic is observed when the magnets are shifted by 27 mm, while the maximum force produced at this value decreases from 370 N to 144 N. For this reason, when the harmonic and generated force values are evaluated together, the best result occurs in the case of 6 mm skewing. As a result, although the maximum force value to be produced by the thrust force decreases when the magnets are shifted by 6 mm, the skew process can be applied to prevent comfort users and motor failures due to the decrease in ripples in the force curves.

References

- [1] A. Barış, M. Güleç, Y. Demir, and M. Aydin, "Electromagnetic Design and Analysis of Permanent Magnet Linear Synchronous Motor," in *Ulusal Elektrik Enerjisi Dönüşümü Kongresi*, Jul. 2017, pp. 1–6, doi: 10.3390/en15155441.
- [2] C. Krämer, A. Kugi, and W. Kemmetmüller, "Modeling of a permanent magnet linear synchronous motor using magnetic equivalent circuits," *Mechatronics*, vol. 76, Jun. 2021, doi: 10.1016/J.MECHATRONICS.2021.102558.
- [3] I. Boldea, M. Pucci, and W. Xu, "Design and Control for Linear Machines, Drives, and MAGLEVs - Part II," *IEEE Trans. Ind. Electron.*, vol. 65, no. 12, pp. 9801–9803, Dec. 2018, doi: 10.1109/TIE.2018.2849761.
- [4] I. Boldea, "Linear Electric Machines, Drives, and MAGLEVs Handbook," *CRC Press*, pp. 1–646, Jan. 2013, doi: 10.1201/B13756.
- [5] I. Eguren, G. Almundoz, A. Egea, G. Ugalde, and A. J. Escalada, "Linear Machines for Long Stroke Applications - A Review," *IEEE Access*, vol. 8, pp. 3960–3979, 2020, doi: 10.1109/ACCESS.2019.2961758.
- [6] S. Chevailler, "(PDF) Comparative study and selection criteria of linear motors," ÉCOLE POLYTECHNIQUE FÉDÉRALE DE LAUSANNE, 2006.
- [7] J. Wang, W. Wang, K. Atallah, and D. Howe, "Comparative studies of linear permanent magnet motor topologies for active vehicle suspension," 2008 *IEEE Veh. Power Propuls. Conf. VPPC* 2008, 2008, doi: 10.1109/VPPC.2008.4677550.
- [8] S. Vaez-Zadeh and A. H. Isfahani, "Multiobjective optimization of air-core linear permanent magnet synchronous motors for improved thrust and low magnet consumption," *ICEMS 2005 Proc. Eighth Int. Conf. Electr. Mach. Syst.*, vol. 1, pp. 226–229, 2005, doi: 10.1109/ICEMS.2005.202517.
- [9] S. G. Lee, S. A. Kim, S. Saha, Y. W. Zhu, and Y. H. Cho, "Optimal structure design for minimizing detent force of PMLSM for a ropeless elevator," *IEEE Trans. Magn.*, vol. 50, no. 1, 2014, doi: 10.1109/TMAG.2013.2277544.
- [10] C. F. Wang, J. X. Shen, Y. Wang, L. L. Wang, and M. J. Jin, "A new method for reduction of detent force in permanent magnet flux-switching linear motors," *IEEE Trans. Magn.*, vol. 45, no. 6, pp. 2843–2846, 2009, doi: 10.1109/TMAG.2009.2018689.
- [11] W. Ullah, F. Khan, N. Ullah, M. Umair, B. Khan, and H. A. Khan, "Comparative Study between C-Core/E-Core SFPMM with Consequent Pole SFPMM," *RAEE 2019 - Int. Symp. Recent Adv. Electr. Eng.*, Aug. 2019, doi: 10.1109/RAEE.2019.8886946.
- [12] Y. Du, G. Yang, L. Quan, X. Zhu, F. Xiao, and H. Wu, "Detent Force Reduction of a C-Core Linear Flux-Switching Permanent Magnet Machine with Multiple Additional Teeth," *Energies* 2017, Vol. 10, Page 318, vol. 10, no. 3, p. 318, Mar. 2017, doi: 10.3390/EN10030318.
- [13] W. Hao and Y. Wang, "Comparison of the Stator Step Skewed Structures for Cogging Force Reduction of Linear Flux Switching Permanent Magnet Machines," *Energies* 2018, Vol. 11, Page 2172, vol. 11, no. 8, p. 2172, Aug. 2018, doi: 10.3390/EN11082172.
- [14] M. Eker, "Adaptive drive element for PV panel cleaning system: linear BLDC motor," *Electr. Eng.*, Nov. 2022, doi: 10.1007/S00202-022-01680-8.
- [15] Poorina Norouzi, "High performance position control of double sided air core linear brushless DC motor," 2015.
- [16] O. Ustun, O. C. Kivanc, and M. S. Mokukcu, "A linear brushless direct current motor design approach for seismic shake tables," *Appl. Sci.*, vol. 10, no. 21, pp. 1–13, Nov. 2020, doi: 10.3390/APP10217618.
- [17] XIN GE, "Simulation of Vibrations in Electrical Machines for Hybrid-electric Vehicles," p. 56 p., 2014.
- [18] J. J. Cai, Q. Lu, X. Huang, and Y. Yes, "Thrust ripple of a permanent magnet LSM with step skewed magnets," *IEEE Trans. Magn.*, vol. 48, no. 11, pp. 4666–4669, 2012, doi: 10.1109/TMAG.2012.2198437.
- [19] X. Z. Huang, J. Li, C. Zhang, Z. Y. Qian, L. Li, and D. Gerada, "Electromagnetic and Thrust Characteristics of Double-sided Permanent Magnet Linear Synchronous Motor Adopting Staggering Primaries Structure," *IEEE Trans. Ind. Electron.*, vol. 66, no. 6, pp. 4826–4836, Jun. 2019, doi: 10.1109/TIE.2018.2860526.

- [20] K. C. Lim, J. K. Woo, G. H. Kang, J. P. Hong, and G. T. Kim, "Detent force minimization techniques in permanent magnet linear synchronous motors," *IEEE Trans. Magn.*, vol. 38, no. 2 I, pp. 1157–1160, 2002, doi: 10.1109/20.996296.
- [21] Y. W. Zhu and Y. H. Cho, "Thrust ripples suppression of permanent magnet linear synchronous motor," *IEEE Trans. Magn.*, vol. 43, no. 6, pp. 2537–2539, 2007, doi: 10.1109/TMAG.2007.893308.